

**QUARK MODEL DESCRIPTION OF THE N-N SYSTEM:
MOMENTUM DISTRIBUTIONS, STRUCTURE FUNCTIONS
AND THE EMC EFFECT**

W. Koepf

School of Physics and Astronomy

Raymond and Beverly Sackler Faculty of Exact Sciences

Tel Aviv University, 69978 Tel Aviv, Israel

L. Wilets

Department of Physics, FM-15

University of Washington, Seattle, WA 98195, USA

(February 26, 1995)

Abstract

We employ a relativistic quark bag picture, the chromo-dielectric soliton model, to discuss the quarks' symmetry structure and momentum distribution in the N - N system. Six-quark clusters are constructed in a constrained mean-field calculation. The corresponding Hamiltonian contains not only an effective interaction between the quarks and a scalar field, which is assumed to parameterize all non-perturbative effects due to the non-linearity of QCD, but also quark-quark interactions mediated through one-gluon-exchange. We also evaluate the quark light-cone distribution functions, characterizing inclusive deep-inelastic lepton scattering, for the nucleon as well as for the six-quark

structures. We find a competition between a softening of the quarks' momenta through the increase of the confinement volume, and a hardening via the admixture of higher symmetry configurations due to the color-electrostatic one-gluon-exchange. These findings suggest an unexpected absence of many-nucleon, multi-quark effects, even though six-quark structures should represent a non-negligible part of the nuclear ground state.

PACS number(s): 24.85.+p, 25.30.Fj, 12.39.Ba

I. INTRODUCTION

In a previous investigation [1], the nucleon-nucleon interaction in terms of quark degrees of freedom was studied. Employing a relativistic quark bag model, the chromo-dielectric soliton model (CDM) [2], six-quark bags were constructed, representing two nucleons at various distances from complete separation to total overlap. Through a constrained mean-field calculation, molecular-type configurations [3] were generated as a function of deformation, and the configuration mixing was evaluated in a coupled channel analysis. The effective Hamiltonian contained not only a scalar background field, but also quark-quark interactions mediated through one-gluon-exchange. The result was an adiabatic nucleon-nucleon potential which was repulsive at short distances, and the origin of which was attributed to the color-electrostatic one-gluon-exchange. In this work, we focus our attention on the quark sub-structure of the N - N system, employing the six-particle wave functions obtained previously.

Well over ten years ago, it had been suggested that the nucleon's radius swells in the nuclear medium, and that overlapping three-quark structures thus have lower momenta than well separated nucleons [4]. It had furthermore been claimed [5], that the clustering of nucleons into six-quark structures can account for the EMC effect [6], i.e., the change of the nucleon's properties in the nuclear environment as observed in deep-inelastic scattering of highly relativistic leptons off nuclei, if one assumes that the quarks' momentum distribution within those clusters is shifted to lower momenta [7].

In the following, we address those issues by means of a detailed analysis of the quark sub-structure of the N - N state, within the model description presented before. We investigate the quark's momentum distribution in six-quark clusters as a function of the inter-nucleon separation, and show that there exists an interesting competition between a softening of the quark's momenta through the increasing confinement volume and a hardening via the admixture of higher configurations, which are usually neglected in investigations in that realm, and that had proven to be important in the study of the N - N potential.

We furthermore evaluate the deep-inelastic structure functions of the nucleon as well as of the six-quark configurations, following the formalism presented by the Adelaide group [8] for the calculation of the nucleon's structure functions from the MIT bag model [9]. In this description, which has since been extended to other non-topological soliton models [10], the twist-two light-front quark distribution functions are calculated from the bag model wave functions at an, *a priori*, unknown renormalization scale, including a Peierls-Yoccoz projection [11] to cure the broken translational invariance and form momentum eigenstates. In order to compare with data, the calculated quark distribution functions are then evolved from the relatively low scale, at which the bag model is expected to be a reasonable approximation to the non-perturbative QCD bound state, to the experimental momentum scale using the non-singlet Altarelli-Parisi evolution equations [12].

The outline of this work is as follows. In Sec. II, we review the model with which we describe the N - N system in terms of quark degrees of freedom. In Sec. III we discuss the symmetry structure and quark momentum distribution of the N - N ground state for various inter-nucleon separations. In Sec. IV, we present the formalism used to calculate the deep-inelastic structure functions for the nucleon, and in Sec. V we extend this technique to the six-quark case. Finally, we summarize and conclude in Sec. VI.

II. THE MODEL

The Lagrangian of the chromo-dielectric, non-topological soliton model [2] is the fundamental QCD Lagrangian supplemented by a scalar field, which parameterizes the bulk of the non-perturbative effects which arise due to the non-linearity of QCD, and which simulates the gluonic condensate and other scalar structures that inhabit the physical vacuum. The model Lagrangian,

$$\mathcal{L} = \bar{\psi}i\gamma^\mu D_\mu\psi + \frac{1}{2}\partial_\mu\sigma\partial^\mu\sigma - U(\sigma) - \frac{1}{4}\kappa(\sigma)F_{\mu\nu}^c F^{\mu\nu c}, \quad (1)$$

is covariant and satisfies chiral symmetry. Here,

$$U(\sigma) = \frac{a}{2!}\sigma^2 + \frac{b}{3!}\sigma^3 + \frac{c}{4!}\sigma^4 + B \quad (2)$$

is the self-interaction energy of the scalar field, $F_{\mu\nu}^c$ is the color- $SU(3)$ gauge field tensor, and

$$\kappa(\sigma) = 1 + \theta(\sigma) \left(\frac{\sigma}{\sigma_v} \right)^2 \left[2 \frac{\sigma}{\sigma_v} - 3 \right] \quad (3)$$

is the color-dielectric function, where σ_v is the scalar field's vacuum expectation value.

Although there is no direct quark-sigma coupling, the quarks still acquire a self-energy through their interactions with the gluon field, and this leads to spatial confinement [2]. Color confinement, on the other hand, arises through the enclosure of the quark cavity by the physical vacuum where the dielectric function goes to zero. The latter also ensures that there are no spurious color Van der Waals forces [13], which trouble many non-relativistic investigations in that realm.

In order to fit the parameters of the model, we construct self-consistent solutions for the nucleon. To simulate spatial confinement, we add an effective coupling between the quarks and the scalar field,

$$\mathcal{L}_{q\sigma} = - g_{eff}(\sigma) \bar{\psi} \psi , \quad (4)$$

with

$$g_{eff}(\sigma) = g_0 \sigma_v \left(\frac{1}{\kappa(\sigma)} - 1 \right) . \quad (5)$$

We employ the coherent state approach and treat the scalar field classically. In addition, gluonic terms are dropped when determining the quark wave functions or the scalar field, and the N- Δ mass splitting is used to adjust the strong coupling constant, α_s .

The six-quark system is then investigated by means of a constrained mean-field calculation for various ‘‘inter-nucleon distances’’ from total separation to complete overlap. Through an external potential [14], quark wave functions are generated as a function of a geometric deformation parameter, α , which for large positive values coincides with the true

inter-nucleon separation, for $\alpha = 0$ corresponds to a spherical bag and for negative α to oblate deformations. We limit ourselves to the lowest states of either parity, $|\sigma\rangle$ and $|\pi\rangle$ in the molecular notation of Ref. [3], with magnetic quantum numbers of $m = \pm 1/2$.

Quark-gluon interactions are treated in the one-gluon-exchange (OGE) approximation, as higher order effects are assumed to be simulated by the scalar field. This yields Abelian gluon field equations,

$$\partial^\mu \left(\kappa(\sigma) [\partial_\mu A_\nu^c - \partial_\nu A_\mu^c] \right) = \frac{g_s}{2} \bar{\psi} \gamma_\nu \boldsymbol{\lambda}^c \psi . \quad (6)$$

Note that the gluon field is explicitly affected by the scalar background through the color-dielectric $\kappa(\sigma)$, and the gluonic propagators are thus evaluated “in medium” [15]. We choose the Coulomb gauge, $\boldsymbol{\nabla} \cdot [\kappa(\sigma) \mathbf{A}^c] = 0$, to deduce the mutual and self-interaction terms, and finally calculate their contribution to the one- and two-body parts of the effective Hamiltonian. The corresponding matrix elements are evaluated by means of “fractional parentage coefficients” [16], and they generate an explicit mixing between the various six-quark configurations. The part of the OGE interactions that arises from the time component of the gluonic field is responsible for color confinement, and the part of the OGE interactions that stems from the spatial components generates the color-magnetic hyperfine interaction which, in turn, produces the N- Δ mass splitting.

In Ref. [1] results were presented for the adiabatic, local N - N potential, obtained in Born-Oppenheimer approximation from the energy difference of a deformed six-quark bag and two well separated, non-interacting nucleons. The isospin-spin channels (TS)=(01) and (TS)=(10), which are compatible with $L = 0$ partial waves, were studied for two different parameter sets, denoted as $f = 3$ and $f = \infty$, adjusted to the standard properties of the nucleon. A purely repulsive central interaction was found with a “soft” core whose maximum varied between 200 and 350 MeV for the two sets. The long and medium range attraction could not be reproduced since it should be attributed to explicit meson exchange and not quark rearrangement, and the “sea” quarks were not included. Also, the non-gluonic contribution of the Hamiltonian was attractive, while the OGE part was dominantly repulsive. In

particular, it was the color-electric one-gluon-exchange, mediated by A_0^c , which lead to the repulsion at small N - N separations, and not the spin-spin color-magnetic hyperfine interaction, which in the literature is quoted [17] as being responsible for the short-range repulsive core. For further details we refer the reader to Ref. [1]. We note that the dynamics of the N - N interaction have been shown to contribute to the repulsion as well [14].

III. SYMMETRY STRUCTURE OF THE SIX-QUARK STATE

The construction of antisymmetric six-quark states is a central part of any study of the N - N system in terms of quarks. Incorporating all possible degrees of freedom – color (C), orbital motion (O), spin (S) and isospin (T) – we employ a classification scheme based on $SU(4)$ spin-isospin symmetry, as introduced by Harvey [16]. For the orbital share of the wave function, we use “molecular orbitals” [3] expressed through spatial single-particle states that are wave functions of a static Hamiltonian, and which in our case are the two lowest orbitals of either parity, $|\sigma\rangle$ and $|\pi\rangle$. If we furthermore restrict ourselves to the isospin-spin channels (TS)=(01) and (TS)=(10), only the following seven configurations, displayed in terms of the Young tableaux characterizing their permutation symmetries,

$$\begin{aligned}
|1\rangle &= |NN\rangle, \\
|2\rangle &= |\Delta\Delta\rangle, \\
|3\rangle &= |CC\rangle, \\
|4\rangle &= |42^+[6]_O [33]_{TS}\rangle, \\
|5\rangle &= |42^+[42]_O [33]_{TS}\rangle, \\
|6\rangle &= |42^+[42]_O [51]_{TS}\rangle, \\
|7\rangle &= |51^+[6]_O [33]_{TS}\rangle,
\end{aligned} \tag{7}$$

contribute significantly to the N - N ground state. The first three contain solely configurations which asymptotically are of the type $|R^3L^3\rangle$, and the other four are of the form

$|R^4L^2 + R^2L^4\rangle$ or $|R^5L + RL^5\rangle$, denoted as 42^+ and 51^+ respectively, where, for general deformation, $|R\rangle$ and $|L\rangle$ are replaced by $|r\rangle$ and $|\ell\rangle$ with

$$|r, \ell\rangle \equiv \frac{|\sigma\rangle \pm |\pi\rangle}{\sqrt{2}}. \quad (8)$$

The pseudo-right/left states, $|r\rangle$ and $|\ell\rangle$, approach $|R\rangle$ and $|L\rangle$ asymptotically, and the latter correspond to a quark centered at the location of either one of the two respective nucleons. All the states in Eq. (7) have color symmetry $[222]_C$, and they mix through the one-gluon-exchange interaction.

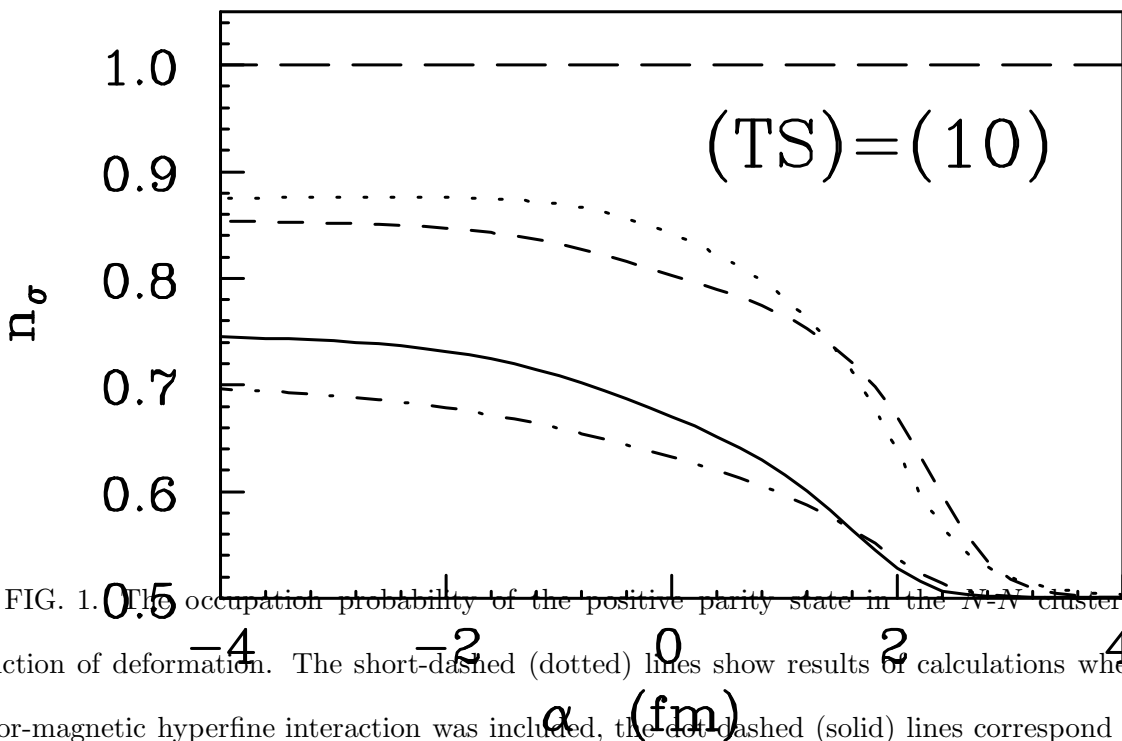


FIG. 1. The occupation probability of the positive parity state in the N^*N^* clusters as a function of deformation. The short-dashed (dotted) lines show results of calculations where the color-magnetic hyperfine interaction was included, the dot-dashed (solid) lines correspond to calculations where also the color-electrostatic force was included, and the long-dashed line refers to a calculation where the OGE was left out altogether. Results are shown for $(TS)=(10)$, and for the parameter sets $f = \infty$ ($f = 3$).

Naïvely one would expect that once the individual bags overlap and the degeneracy between the single-particle states vanishes, all quarks occupy the lowest spatial orbital, and this hypothesis is an implicit ingredient to all works where a lowering of the quarks' momenta in six-quark clusters is discussed [5]. To test that assumption, we show in Fig. 1

the probability of the quarks in the N - N clusters to occupy the lowest single-particle state, $|\sigma\rangle$,

$$n_\sigma = \frac{1}{6} \langle 6q | \hat{a}_\sigma^\dagger \hat{a}_\sigma | 6q \rangle , \quad (9)$$

where the six-quark ground state was obtained while including different parts of the one-gluon-exchange contribution in the diagonalization of the effective Hamiltonian.

The quantity n_σ is shown as a function of the parameter α , which characterizes the deformation of the external potential used to generate the single quark wave functions, and which for large positive α coincides with the true inter-nucleon separation, r_{NN} . Note that the spherical configuration, $\alpha = 0$, corresponds to a still finite inter-nucleon separation, and that $r_{NN} \rightarrow 0$ is approached for oblate deformations, i.e., for $\alpha < 0$.

We observe that only if the gluonic interaction is neglected completely can all quarks move into the lowest single-particle orbital. The inclusion of the one-gluon-exchange, and the channel-coupling it generates, leads to a non-negligible occupation of higher states, of the form $|\sigma^4\pi^2\rangle$ and $|\sigma^2\pi^4\rangle$, in particular if not only the color-magnetic hyperfine but also the color-electrostatic interaction is considered. The latter is frequently neglected in investigations in that realm, and it had proven to be essential for obtaining the short-range repulsion in the investigation of the N - N interaction in Ref. [1]. Actually, neglect of the gluonic interactions in a *dynamical* calculation would lead to $n_\sigma = 1/2$. This is because $n_\sigma = 1/2$ for well separated nucleons, i.e., the $|NN\rangle$ state, and only gluonic interactions (or Coriolis mixing) could change the occupation of the individual orbitals in, e.g., a time-dependent mean-field calculation.

In Fig. 2 we show the single quark's average momentum,

$$\langle k \rangle \equiv \frac{1}{6} \sqrt{\langle 6q | \hat{k}^2 | 6q \rangle} , \quad (10)$$

as a function of the deformation of the six-quark clusters, and again employing different shares of the one-gluon-exchange contribution to the effective Hamiltonian. If the one-gluon-exchange is neglected and all quarks are assumed to occupy the lowest single-particle

orbital, i.e., $|6q\rangle \sim |\sigma^6\rangle$, the increase in the size of the confinement volume leads to a strong decrease of the quark's momenta as soon as the nucleonic bags overlap considerably. As mentioned earlier, this observation is at the heart of the numerous investigations where either the swelling of the nucleon in the nuclear medium [4] or the contribution of many-nucleon, multi-quark effects to nuclear observables is discussed [5].

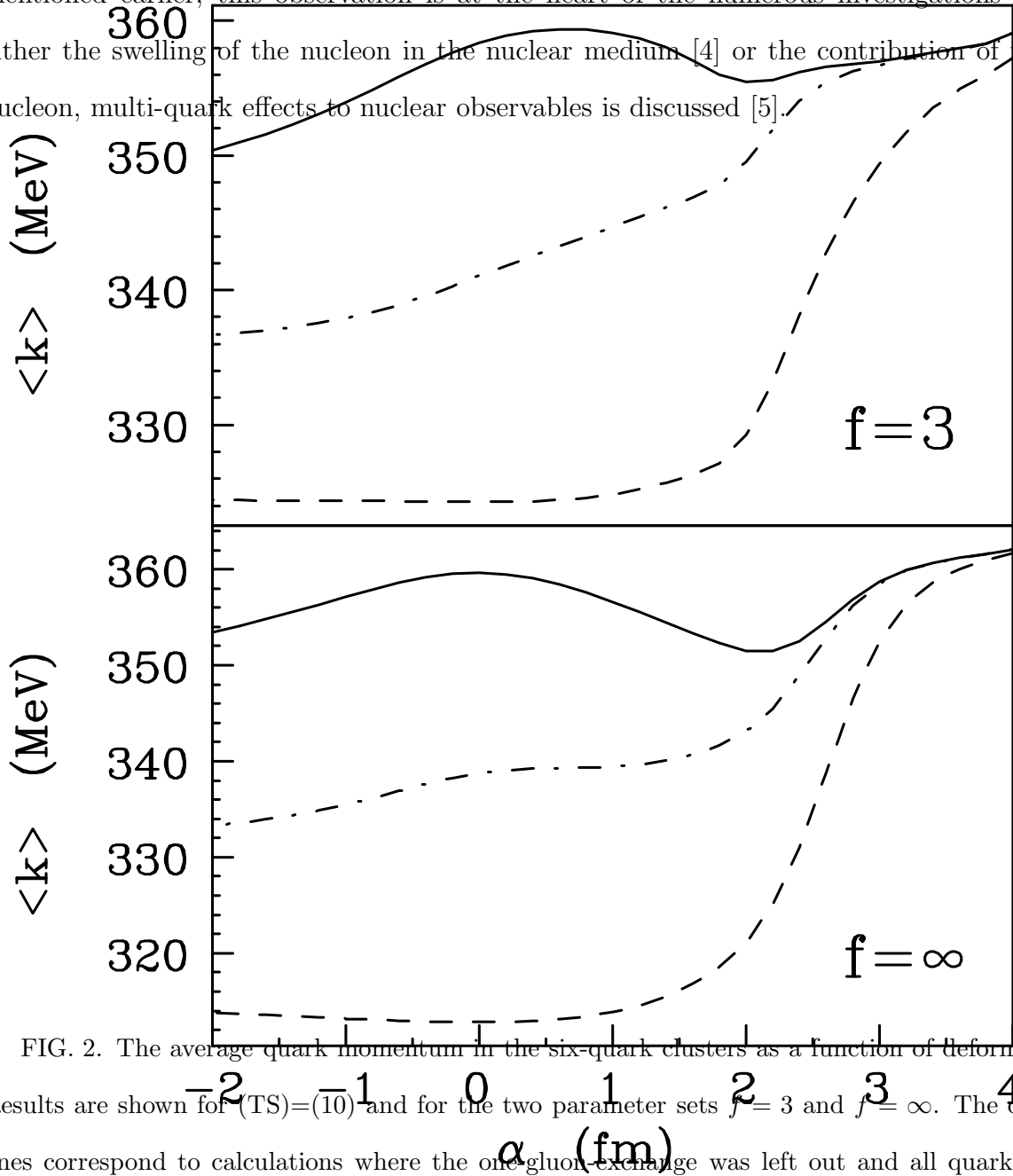


FIG. 2. The average quark momentum in the six-quark clusters as a function of deformation. Results are shown for $(TS)=(\bar{10})$ and for the two parameter sets $f=3$ and $f=\infty$. The dashed lines correspond to calculations where the one-gluon-exchange was left out and all quarks were assumed to occupy the lowest orbital, the dot-dashed lines show the results of calculations where the color-magnetic hyperfine interaction was included, and the solid lines refer to calculations where also the color-electrostatic interaction was accounted for.

However, the inclusion of the one-gluon-exchange interaction leads to an admixture of

higher states, as has been depicted in Fig. 1, and hence also to a hardening of the quarks' average momentum. In particular, when not only the color-magnetic hyperfine interaction but also the color-electrostatic share of the OGE is considered, the aforementioned hardening almost counterbalances the softening from the increase in the size of the confining volume. This cancellation points towards an unexpected absence of multi-quark effects, even if six-quark structures represent a non-negligible part of the nuclear ground state.

IV. DEEP-INELASTIC STRUCTURE FUNCTIONS

As one the most prominent areas in which six-quark effects are supposed to play a dominant role [5] is the EMC effect, i.e., the change of the properties of the nucleon in the nuclear environment as observed in deep-inelastic lepton scattering, we evaluate in the following the unpolarized, deep-inelastic structure functions of the nucleon as well as of the six-quark clusters.

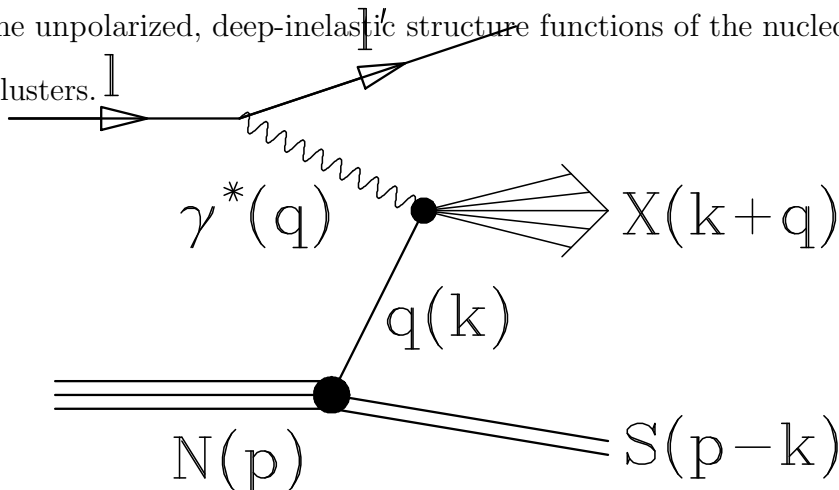


FIG. 3. Inclusive scattering of a high-energy lepton from a nucleonic target. The virtual photon, γ^* , is absorbed by a quark, q , in the target nucleon, N , leaving behind a spectator, S , and producing an undetected final state, X . The quantities in brackets are the particles' momenta.

Consider the inclusive scattering of a high-energy lepton from a nucleonic target, as depicted in Fig. 3. We assume that a spacelike virtual photon is absorbed by a quark with momentum k in the target nucleon, leaving behind a “spectator” and producing an arbitrary undetected final state. In the laboratory frame, the relevant momenta are

$$q = (\nu, \mathbf{0}_\perp, -|\mathbf{q}|) , \quad (11a)$$

$$p = (M, \mathbf{0}) , \quad (11b)$$

$$k = (k_0, \mathbf{k}) , \quad (11c)$$

where M is the nucleon mass. It is customary to characterize the spacelike photon by means of its virtuality, $Q^2 \equiv |\mathbf{q}|^2 - \nu^2$, and through the Bjorken scaling variable, $x_B \equiv \frac{Q^2}{2M\nu}$. In the following, we are only interested in the kinematic limit where $Q^2 \rightarrow \infty$ while x_B remains finite. Transforming into the Breit (or infinite-momentum) frame, where the energy of the exchanged virtual photon vanishes, we find to leading order in an expansion in $1/Q^2$,

$$q' = (0, \mathbf{0}_\perp, -Q) , \quad (12a)$$

$$p' \approx \left(\frac{Q^2 + 2M^2 x_B^2}{2Qx_B}, \mathbf{0}_\perp, \frac{Q}{2x_B} \right) , \quad (12b)$$

$$k' \approx \left(\frac{Q^2(k_0 + k_z) + 2M^2 x_B^2 k_0}{2MQx_B}, \mathbf{k}_\perp, \frac{Q^2(k_0 + k_z) + 2M^2 x_B^2 k_z}{2MQx_B} \right) . \quad (12c)$$

The quark's light-cone momentum fraction x is defined as the ratio of the \hat{z} -components of the momenta of the struck quark and the target nucleon in the Breit frame, i.e.,

$$x \equiv \frac{k'_z}{p'_z} \approx \frac{k_0 + k_z}{M} \approx x_B , \quad (13)$$

where the second and third equalities are valid to leading order in $1/Q^2$ only.

According to Jaffe [18], the leading-twist contribution to the quark distribution functions, which characterize the probability to find a quark of flavor f carrying a fraction x of the target's light-cone momentum, may be written as

$$q_f(x) = \sum_S \delta(x - k_+/M) |\langle S | \hat{\psi}_{+,f}(0) | N \rangle|^2 , \quad (14)$$

where the sum runs over all possible intermediate spectator states, and where k_+ is the plus-component of the struck quark's momentum in the laboratory frame, $k_+ = k_0 + k_z$. Employing this equation, the nucleon's structure functions can, in principle, be calculated from any phenomenological, low-energy model. The respective formalism was developed for a evaluation of the nucleon's structure functions from the MIT bag model [8], and it

has since been extended to other non-topological soliton models [10], and to the nuclear structure functions [19,20]. In the sum in Eq. (14), we restrict ourselves to a single two-quark intermediate spectator state, which we furthermore assume to be on its mass-shell with mass M_S . This, in turn, fixes the struck quark's energy to $k_0 = M - \sqrt{M_S^2 + |\mathbf{k}|^2}$. Obviously, the truncation of the sum in Eq. (14) after only one term is a very strong approximation, and we continue to discuss its validity in the remainder of this section.

This then yields

$$q_f(x) = \frac{1}{(2\pi)^3} \sum_m \langle \mu | P_{f,m} | \mu \rangle \int d^3\mathbf{k} \frac{\phi_2(|\mathbf{k}|)}{\phi_3(0)} |\psi_{+,f,m}(\mathbf{k})|^2, \quad (15)$$

where $|\mu\rangle$ is the $SU(6)$ spin-flavor wave function of the initial nucleon, $P_{f,m}$ is a projector onto flavor f and helicity m , and

$$|\psi_{+,f,m}(\mathbf{k})|^2 = \delta(x - k_+/M) \int d^3\mathbf{r} \int d^3\mathbf{r}' \psi_{f,m}^\dagger(\mathbf{r}) \frac{1 + \alpha_z}{2} \psi_{f,m}(\mathbf{r}') e^{i\mathbf{k}(\mathbf{r}-\mathbf{r}')} \quad (16)$$

is the Fourier transform of the twist-two contribution to the connected matrix element of the current-current correlator. The δ -function, which fixes the plus-component of the struck quark's momentum, can be rewritten as

$$\delta(x - k_+/M) = \frac{M}{|\mathbf{k}|} \delta\left(\cos\theta_k - \frac{\sqrt{M_S^2 + |\mathbf{k}|^2} - M(1-x)}{|\mathbf{k}|}\right), \quad (17)$$

and it yields a lower limit in the integration over the struck quark's three-momentum, i.e., $|\mathbf{k}| \geq k_{min}$, where

$$k_{min} = \left| \frac{M^2(1-x)^2 - M_S^2}{2M(1-x)} \right|. \quad (18)$$

From this we observe that the quark distribution has support not only for $0 \leq x \leq 1$, but also for negative x . However, as shown by Jaffe [18], there are other semi-connected diagrams, which are not included into our formalism, and which exactly cancel the contributions for negative x . We hence proceed and simply neglect that spurious domain.

In Eq. (15) we also included a Peierls-Yoccoz [11] projection onto momentum eigenstates, expressed by means of the Hill-Wheeler overlap functions,

$$\phi_n(|\mathbf{k}|) = 4\pi \int_0^\infty dR R^2 j_0(|\mathbf{k}|R) T^n(R) , \quad (19)$$

with

$$T(R) = \int d^3\mathbf{r} \psi_{f,m}^\dagger(\mathbf{r}) \psi_{f,m}(\mathbf{r} + \mathbf{R}) , \quad (20)$$

and where $n = 2$ for the intermediate di-quark state, and $n = 3$ for the initial nucleon.

As noticed first by Close and Thomas [21], the mass of the spectator state depends on whether the latter is in a spin singlet or in a spin triplet, due to the one-gluon-exchange. This is usually built into model descriptions of that type by assigning different masses, $M_S^{S=0}$ and $M_S^{S=1}$, to the intermediate di-quark singlet and triplet states, and it has been demonstrated [8] that this yields a satisfactory description of the quark distribution functions' flavor and spin dependence. As in this work, we are only interested in flavor and spin averaged distributions, we neglect this effect in the following, and simply set

$$M_S = M - \epsilon , \quad (21)$$

where ϵ is the quark's single particle energy, which has the values $\epsilon = 340$ MeV ($f = 3$) and $\epsilon = 335$ MeV ($f = \infty$) for the two parameter sets.

Previously, we constructed self-consistent solutions for the nucleon. We used those calculations to fit the parameters of our model, a , b and c in $U(\sigma)$ of Eq. (2), g_0 in g_{eff} of Eq. (5) and the strong coupling constant α_s , and we presented solutions for $f \equiv b^2/ac = 3$ and $f = \infty$. In the following, we evaluate Eq. (15) with the respective $s_{1/2}$ quark wave functions,

$$\psi_m(\mathbf{r}) = \begin{pmatrix} f(r) \\ i\boldsymbol{\sigma} \cdot \hat{\mathbf{r}} g(r) \end{pmatrix} \chi_m^{[1/2]} . \quad (22)$$

This yields

$$q(x) = \frac{M}{\pi^2} \int_{k_{min}}^\infty d|\mathbf{k}| |\mathbf{k}| \frac{\phi_2(|\mathbf{k}|)}{\phi_3(0)} \left[I_0(|\mathbf{k}|)^2 + 2I_0(|\mathbf{k}|)I_1(|\mathbf{k}|) \cos \theta_k + I_1(|\mathbf{k}|)^2 \right] \quad (23)$$

for the flavor and spin averaged quark distribution function. The term $\cos \theta_k$ is fixed via Eq. (17), k_{min} is given in Eq. (18), and with

$$I_0(|\mathbf{k}|) = \sqrt{\pi} \int dr r^2 f(r) j_0(|\mathbf{k}|r) , \quad (24a)$$

$$I_1(|\mathbf{k}|) = \sqrt{\pi} \int dr r^2 g(r) j_1(|\mathbf{k}|r) . \quad (24b)$$

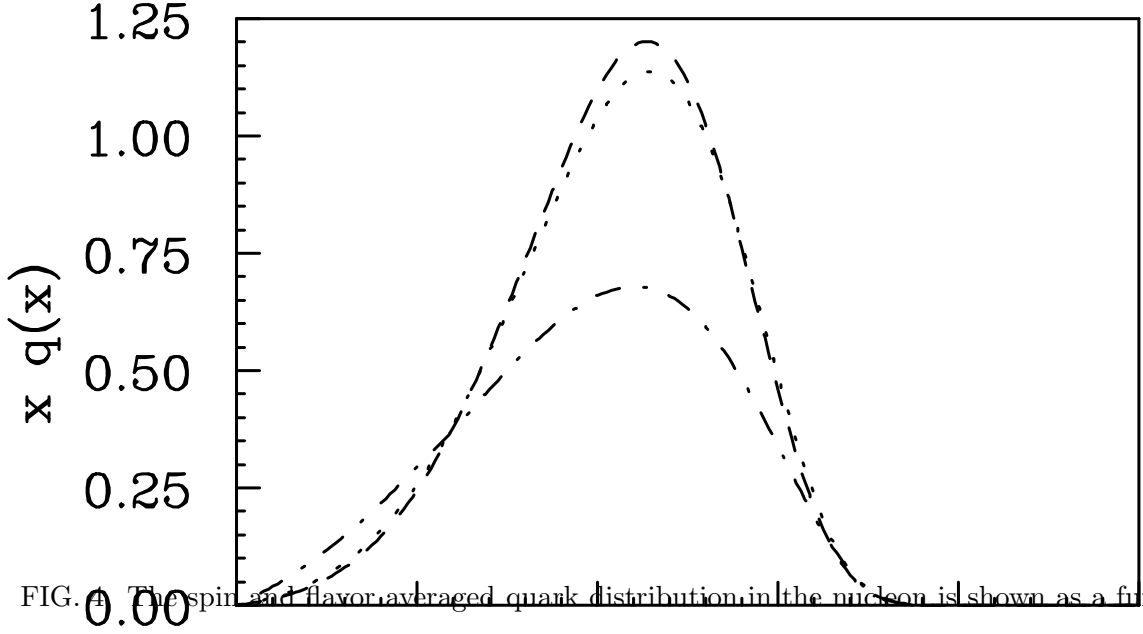


FIG. 4. The spin and flavor averaged quark distribution in the nucleon is shown as a function of the struck quark's momentum fraction. Results are displayed for the DD for the parameter sets $f = 3$ (dashed line) and $f = \infty$ (dotted line), and for the MIT bag model with a bag radius of $R = 1$ fm (dot-dashed line).

In Fig. 4, we show $x q(x)$ for the two parameter sets and for the MIT bag model for a bag radius of $R = 1$ fm and setting $\epsilon = \frac{M}{4}$ in accordance with the bag virial theorem. Note that due to the truncation of the sum over all possible intermediate spectators after only a single di-quark state, the quark distribution functions do not satisfy the normalization condition, i.e.,

$$\int_0^1 dx q(x) \neq 1 . \quad (25)$$

The violation is much larger for the MIT bag model ($\approx 17\%$) than for the chromo-dielectric soliton model ($\approx 2\%$), and it is usually cured by adding a phenomenological term, $\sim (1-x)^7$, which is supposed to parameterize the contribution from four-particle intermediate states [8,10]. That term is then scaled such that the normalization requirement is fulfilled. As we are only interested in a qualitative discussion, and as the deviation is anyhow minute for the

CDM, we do not adopt this prescription. With this, we restrict ourselves to a pure valence quark picture and neglect all “sea” contributions.

We see from Fig. 4, that the MIT bag model leads to a wider light-cone momentum distribution. This reflects the effect of the sharp cut-off at the surface of the MIT bag, which, in turn, yields momentum-components in the quark wave function that extend to very high momenta and to a broad peak for $xq(x)$. Note that the location of the peak is determined by the mass of the spectator state through k_{min} of Eq. (18), which suggests that $q(x)$ is maximal for $x \approx 1 - M_S/M$.

To compare our results with experimental data, the calculated quark distribution functions are evolved from the relatively low scale, $\mu < 1$ GeV, at which the bag model is expected to be a reasonable approximation to non-perturbative QCD, to the experimental momentum scale, $Q^2 > 5$ GeV², using the non-singlet Altarelli-Parisi evolution equations [12]. The bag model scale is then fixed by requiring an optimal fit to a recent parameterization [22] of the experimental iso-singlet valence quark distribution in the nucleon at $Q^2 = 10$ GeV². We use next-to-leading-order QCD evolution in the modified minimal subtraction scheme (\overline{MS}) with $\Lambda_{QCD} = 213$ MeV for four flavors [23]. The corresponding results are shown in Fig. 5, and we find $\mu = 0.33$ GeV for the chromo-dielectric soliton model and $\mu = 0.38$ GeV for the MIT bag model.

Up to $x \approx 0.5$ both models yield a reasonable fit to the data-based parameterization. Note that large x at high Q^2 correspond to even larger x before the evolution, i.e., at the scale where the bag model is valid, and hence to very high quark momenta, for which both the bag model and the non-relativistic Peierls-Yoccoz projection become very questionable. The smallness of the bag model scale is also a concern, due to the question of the applicability of perturbative QCD. We comfort ourselves, however, with the realization that we are ultimately only interested in a qualitative discussion of a ratio of structure functions, which should display much weaker Q^2 dependence.

We furthermore observe that the peaks of the distributions are generally higher and/or at larger values of x than the data. This deviation, which was also observed in Ref. [10], is more

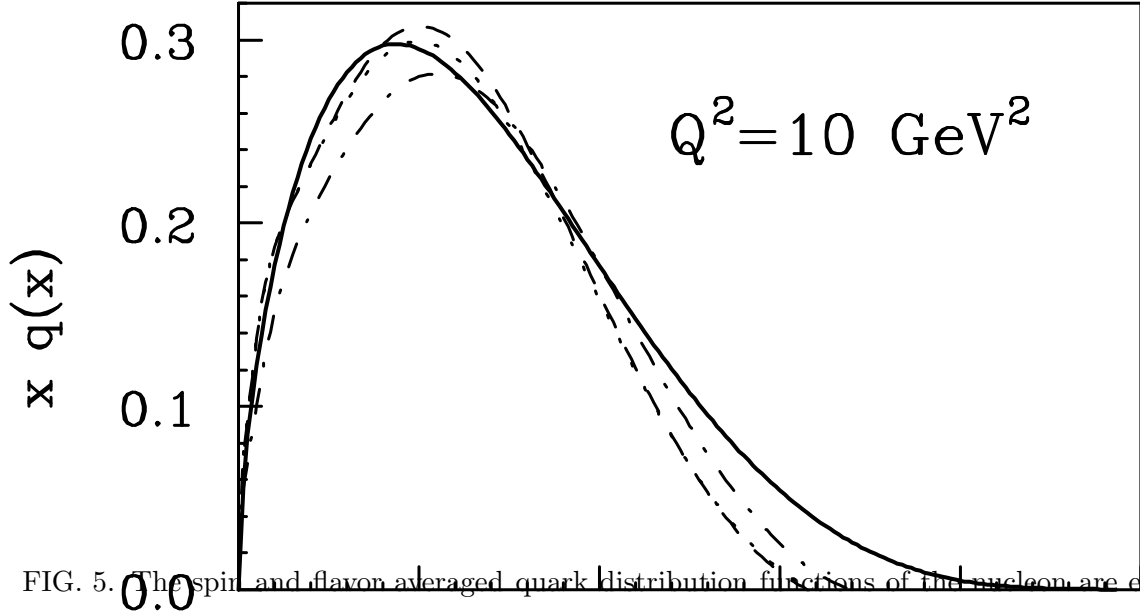


FIG. 5. The spin and flavor averaged quark distribution functions of the nucleon are evolved to a momentum scale of $Q^2 = 10 \text{ GeV}^2$. Results are shown for the chromo-dielectric soliton model and the MIT bag model, and they are compared with recent parameterization of experimental data [22] (solid line). The remaining labeling is the same as in Fig. 4.

pronounced for the chromo-dielectric soliton than for the MIT bag model, and even better fits were obtained for the latter for smaller bag radii of $R \approx 0.6 \dots 0.8 \text{ fm}$ [8]. This shows that deep-inelastic scattering data point towards higher quark momenta and thus smaller bags. As the parameters of the model, and hence the size of the bag, were adjusted to fit standard nucleonic properties, i.e., the mass, the charge radius and the magnetic moment, latter deviation suggests that inclusive deep-inelastic scattering does not probe the “average nucleon” but is only sensitive to a “small-size” component in the nucleon’s wave function. Work in that direction is currently in progress [24].

V. STRUCTURE FUNCTIONS OF SIX-QUARK CLUSTERS

Previous estimates of the quark light-cone momentum distribution in six-quark clusters were based on dimensional counting rules [7], valid in the limit $x \rightarrow 1$, and on Regge arguments [25] for low x . Here, we calculate the quark distribution of six-quark structures in the framework of a model whose parameters were adjusted to yield an optimal description

of the corresponding quantity for the nucleon.

The different target mass, M_{6q} instead of M , leads to trivial modifications in the definition of the struck quark's momentum fraction,

$$x \equiv \frac{k'_z}{p'_z} \approx \frac{k_0 + k_z}{M_{6q}} \approx \frac{M}{M_{6q}} x_B , \quad (26)$$

and the quark distribution function,

$$q_f^{6q}(x) = \sum_S \delta(x - k_+/M_{6q}) |\langle S | \hat{\psi}_{+,f}(0) | 6q \rangle|^2 . \quad (27)$$

Employing the same approximations than in the last section, we truncate this sum after a single spectator state, which we assume to be a five-quark system that is on its mass shell with mass M_S .

In the following, we restrict ourselves to spherically symmetric six-quark bags, i.e., to $\alpha = 0$. The six-quark state can be expressed through terms of the form $|\sigma^p \pi^{6-p} [f]_O [f']_{TS}\rangle$, with $p \in \{0, 2, 4, 6\}$ and where $[f]_O$ and $[f']_{TS}$ denote Young symmetries. As we are interested in spin and isospin averaged quark distributions only, the latter are irrelevant in the following, and the six-quark cluster can be represented as,

$$|6q\rangle = a_6 |\sigma^6\rangle + a_4 |\sigma^4 \pi^2\rangle + a_2 |\sigma^2 \pi^4\rangle + a_0 |\pi^6\rangle , \quad (28)$$

where $|\sigma^p \pi^{6-p}\rangle$ denotes a system with p quarks in the positive parity state $|\sigma\rangle$, and $6-p$ quarks in the negative parity state $|\pi\rangle$. Note that the single-particle states evolve to $|\sigma\rangle \rightarrow |s_{1/2}\rangle$ and $|\pi\rangle \rightarrow |p_{3/2}\rangle$ for $\alpha = 0$. As the terms in the sum in Eq. (28) add incoherently for the deep-inelastic process, we can write

$$q_{6q}(x) = |a_6|^2 q_{60}^{6q}(x) + |a_4|^2 q_{42}^{6q}(x) + |a_2|^2 q_{24}^{6q}(x) + |a_0|^2 q_{06}^{6q}(x) \quad (29)$$

for the quark distribution of the six-quark clusters, and where $q_{pq}^{6q}(x)$ is the distribution function of the configuration $|\sigma^p \pi^q\rangle$. The latter obtain incoherent contributions from processes where a quark is knocked out of either single-particle orbital,

$$q_{pq}^{6q}(x) = \frac{p}{p+q} q_{pq\sigma}^{6q}(x) + \frac{q}{p+q} q_{pq\pi}^{6q}(x) , \quad (30)$$

where, in generalization of Eq. (23),

$$q_{pq\sigma}^{6q}(x) = \frac{M_{6q}}{\pi^2} \int_{k_{min}^{6q}}^{\infty} d|\mathbf{k}||\mathbf{k}| \frac{\phi_{p-1q}(|\mathbf{k}|)}{\phi_{pq}(0)} \mathcal{I}^{\sigma}(|\mathbf{k}|, \cos \theta_k^{6q}) , \quad (31a)$$

$$q_{pq\pi}^{6q}(x) = \frac{M_{6q}}{\pi^2} \int_{k_{min}^{6q}}^{\infty} d|\mathbf{k}||\mathbf{k}| \frac{\phi_{pq-1}(|\mathbf{k}|)}{\phi_{pq}(0)} \frac{3 \cos^2 \theta_k^{6q} + 1}{2} \mathcal{I}^{\pi}(|\mathbf{k}|, \cos \theta_k^{6q}) , \quad (31b)$$

and where

$$\mathcal{I}^{\sigma,\pi}(|\mathbf{k}|, \cos \theta_k^{6q}) = I_0^{\sigma,\pi}(|\mathbf{k}|)^2 + 2I_0^{\sigma,\pi}(|\mathbf{k}|)I_1^{\sigma,\pi}(|\mathbf{k}|) \cos \theta_k^{6q} + I_1^{\sigma,\pi}(|\mathbf{k}|)^2 , \quad (32)$$

with

$$I_0^{\sigma,\pi}(|\mathbf{k}|) = \sqrt{\pi} \int dr r^2 f_{\sigma,\pi}(r) j_{l_{\sigma,\pi}}(|\mathbf{k}|r) , \quad (33a)$$

$$I_1^{\sigma,\pi}(|\mathbf{k}|) = \sqrt{\pi} \int dr r^2 g_{\sigma,\pi}(r) j_{l_{\sigma,\pi}+1}(|\mathbf{k}|r) . \quad (33b)$$

We employed single quark wave functions of the form

$$\psi_{\sigma,\pi\pm\frac{1}{2}}(\mathbf{r}) = \begin{pmatrix} f_{\sigma,\pi}(r) \\ i\boldsymbol{\sigma} \cdot \hat{\mathbf{r}} g_{\sigma,\pi}(r) \end{pmatrix} Y_{j_{\sigma,\pi} l_{\sigma,\pi}}^{\pm\frac{1}{2}}(\boldsymbol{\Omega}) , \quad (34)$$

where $j_{\sigma} = 1/2$, $j_{\pi} = 3/2$, $l_{\sigma} = 0$ and $l_{\pi} = 1$, and with the Hill-Wheeler overlap kernels,

$$\phi_{pq}(|\mathbf{k}|) = 4\pi \int_0^{\infty} dR R^2 j_0(|\mathbf{k}|R) T_{\sigma}^p(R) T_{\pi}^q(R) , \quad (35)$$

where

$$T_{\sigma,\pi}(R) = \int d^3\mathbf{r} \psi_{\sigma,\pi\pm\frac{1}{2}}^{\dagger}(\mathbf{r}) \psi_{\sigma,\pi\pm\frac{1}{2}}(\mathbf{r} + \mathbf{R}) . \quad (36)$$

The term $\cos \theta_k^{6q}$ is given by

$$\cos \theta_k^{6q} = \frac{\sqrt{M_S^2 + |\mathbf{k}|^2} - M_{6q}(1-x)}{|\mathbf{k}|} , \quad (37)$$

and the lower limit in the integration over the struck quark's three-momentum is

$$k_{min}^{6q} = \left| \frac{M_{6q}^2(1-x)^2 - M_S^2}{2M_{6q}(1-x)} \right| . \quad (38)$$

In Fig. 6 we display the quark light-cone distributions in the six-quark clusters which we obtain when including different parts of the one-gluon-exchange interaction when diagonalizing the effective Hamiltonian. In particular, in calculation (I) the OGE was left out altogether, in calculation (II) only the color-magnetic hyperfine interaction was considered, and in calculation (III) also the color-electrostatic force was included. The distribution functions are again evolved from the bag model scale, $\mu = 0.33$ GeV, to the experimental scale, $Q^2 = 10$ GeV². The quark distributions, $x q_{6q}(x)$, are shown as functions of the Bjorken scaling variable, x_B , identifying the struck quark's momentum fraction through $x = \frac{M}{M_{6q}} x_B$, and they are compared with the corresponding quantity for the nucleon, $x q(x)$, for which $x = x_B$. For clarity, we restrict ourselves to one parameter set only.

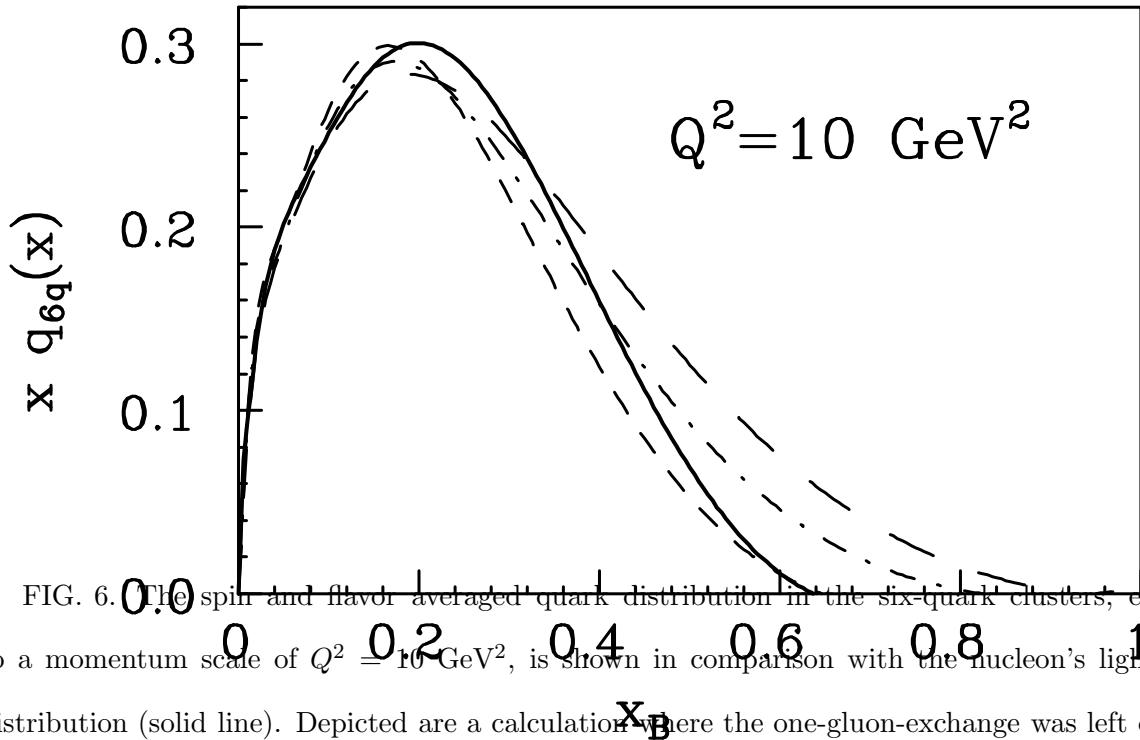


FIG. 6. The spin and flavor averaged quark distribution in the six-quark clusters, evolved to a momentum scale of $Q^2 = 10$ GeV², is shown in comparison with the nucleon's light-cone distribution (solid line). Depicted are a calculation where the one-gluon-exchange was left out altogether (short-dashed line), a calculation where only the color-magnetic hyperfine interaction was included (dot-dashed line), and a calculation where also the color-electrostatic force was accounted for (long-dashed line). Results are shown for $(TS)=(10)$ and $f = \infty$.

For the mass of the six-quark state, M_{6q} , we write

$$M_{6q} = 2M + V_{ad}(\alpha = 0), \quad (39)$$

where $V_{ad}(\alpha = 0)$ is the energy difference of a spherically symmetric six-quark bag and two non-interacting nucleons, which is -338 MeV for calculation (I), -69 MeV for calculation (II) and $+175$ MeV for calculation (III). The mass of the spectator is set to

$$M_S = M_{6q} - \epsilon , \quad (40)$$

where ϵ is the struck quarks's single particle energy, which takes the values 272 (413) MeV for the $|\sigma\rangle$ ($|\pi\rangle$) state.

We observe that only if the one-gluon-exchange interaction is neglected, the distribution of the quarks in the six-quark clusters is shifted to lower x , as has been assumed frequently in the literature [5,7,26,27]. As already pointed out in Sec. III, the reason for that softening of the quarks' momenta is the increase of the confining volume. However, when the one-gluon-exchange interaction is included, the channel-coupling it generates leads to an admixture of higher configurations, and hence to a hardening of the quarks' average momentum, which competes with the aforementioned shift to lower x . As can be seen from Fig. 6, this competition persists in the deep-inelastic domain, and the conclusions we draw for the non-relativistic quark momentum distribution apply to the light-cone distributions as well. This effect is even more pronounced if also the color-electrostatic part of the OGE interaction is considered.

To further elaborate that point, we plot in Fig. 7 the “structure function ratio” [26]

$$R(x_B) = (1 - f) + f \frac{x q_{6q}(x) \Big|_{x=\frac{M}{M_{6q}}x_B}}{x q(x) \Big|_{x=x_B}} , \quad (41)$$

which has been presented in the literature [26,27] for a quantitative description of the EMC effect in the framework of the quark cluster model [5], together with experimental deep-inelastic nuclear cross-section ratios, $F_2^{Fe}(x_B)/F_2^D(x_B)$, of iron over deuterium [28,29].

The quark cluster model is based on the assumption that in finite nuclei there exists a non-negligible probability, f , for the nucleons to break up into six-quark structures [5]. If the quark's light-cone distribution in the six-quark clusters is different from that in a free nucleon, also the nuclear structure functions, $F_2^A(x_B)$, will be different from their nucleonic

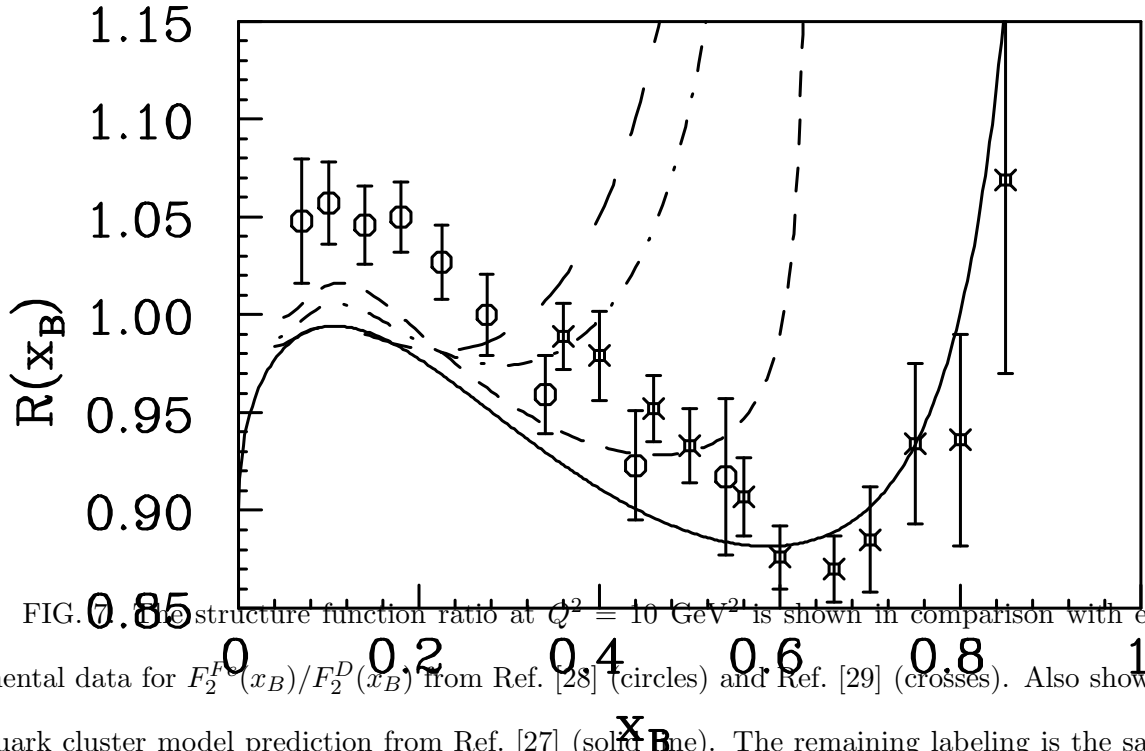


FIG. 7. The structure function ratio at $Q^2 = 10 \text{ GeV}^2$ is shown in comparison with experimental data for $F_2^{Fe}(x_B)/F_2^D(x_B)$ from Ref. [28] (circles) and Ref. [29] (crosses). Also shown is a quark cluster model prediction from Ref. [27] (solid line). The remaining labeling is the same as in Fig. 6.

counterpart, with $R(x_B) \approx F_2^A(x_B)/F_2^D(x_B)$ [26,27]. As suggested in Refs. [26] and [27], we use a probability of $f = 0.30$ for the formation of six-quark clusters in the Fe nucleus.

If we neglect the one-gluon-exchange, the quark distribution in the six-quark structures is shifted to lower x through the larger confinement volume, and we observe a “EMC like” behavior of the ratio $R(x_B)$, as can be seen from the short-dashed line in Fig. 7 which qualitatively follows the data. However, if the one-gluon-exchange is included, the softening of the quark distributions is cancelled by the admixture of higher and harder configurations, and the respective ratios $R(x_B)$ are very different from the data. This is especially the case if we include the color-electrostatic share of the one-gluon-exchange, which had proven to be crucial for a correct description of the short-range repulsive core of the N - N interaction.

VI. CONCLUSIONS

We have continued our study of the two-nucleon system in terms of quark degrees of freedom, shifting the focus of our attention from the adiabatic potential to the quark-

substructure. Employing a relativistic quark bag model, which yields spatial as well as color confinement, we have constructed six-quark states which are confined in a deformed bag-like mean field through an effective non-linear interaction with a self-consistently determined scalar background field. The corresponding Hamiltonian includes also quark-quark interactions generated through one-gluon-exchange, and when evaluating the gluonic propagators, which mediate that interaction, the inhomogeneity and deformation of the dielectric medium were taken into account. Six-quark molecular-type configurations were generated as a function of deformation, and the effective Hamiltonian was diagonalized in a coupled channel analysis and while accounting for different shares of the one-gluon-exchange interaction.

The symmetry structure and the quarks' non-relativistic momentum distribution in the six-quark state were discussed, and it was shown, that there exists an interesting competition between a softening of the quarks' momenta through the increase in the size of the confining volume, and a hardening via the admixture of higher symmetry configurations.

Then, the spin and isospin averaged deep-inelastic structure functions of the nucleon as well as the six-quark configurations were evaluated following the formalism presented by the Adelaide group. In detail, the twist-two light-front quark distribution functions were calculated from the bag model wave functions including a Peierls-Yoccoz projection to cure the broken translational invariance. The quark distribution functions were then evolved from the relatively low scale, at which the bag model is expected to be a reasonable approximation to non-perturbative QCD, to the experimental momentum scale, using the non-singlet Altarelli-Parisi evolution equations, and the bag model scale was adjusted so that the evolved quark distribution functions agree well with experimental data. The corresponding light-cone distributions of the six-quark structures were then predicted, and finally a "structure function ratio", proposed previously in the framework of the quark cluster model, was presented.

It was shown that this ratio displays the typical behavior that characterizes the EMC effect only if the one-gluon-exchange interaction is neglected. However, the underlying shift of the six-quark distribution functions to lower x , which is usually assumed in investigations

in that realm, is cancelled completely by the admixture of higher and harder configurations if the one-gluon-exchange interaction is included. As the latter was essential in reproducing the short-range repulsive core of the adiabatic N - N potential, the naïve picture of a softening of the quark's distribution functions in the six-quark clusters due to the increase of the confining volume, which was put forward e.g., in the framework of the quark cluster model, is put into question.

ACKNOWLEDGMENTS

We wish to thank J.M. Eisenberg, L.L. Frankfurt, Fl. Stancu and S. Pepin for many useful discussions. We also thank R. Kobayashi, M. Konuma and S. Kumano as well as the CTEQ Collaboration for providing us with their FORTRAN codes. This work was supported in part by the U.S. Department of Energy, and by the MINERVA Foundation of the Federal Republic of Germany.

REFERENCES

- [1] W. Koepf, L. Wilets, S. Pepin and Fl. Stancu, Phys. Rev. **C50**, 614 (1994).
- [2] G. Fai, R.J. Perry and L. Wilets, Phys. Lett. **B208**, 1 (1988); G. Krein, P. Tang, L. Wilets and A.G. Williams, Phys. Lett. **B212**, 362 (1988) and Nucl. Phys. **A523**, 548 (1991).
- [3] Fl. Stancu and L. Wilets, Phys. Rev. **C36**, 726 (1987); Phys. Rev. **C38**, 1145 (1988); Phys. Rev. **C40**, 1901 (1989).
- [4] J.V. Noble, Phys. Rev. Lett. **46**, 412 (1981) and Phys. Lett. **B178**, 285 (1986).
- [5] H. Pirner and J.P. Vary, Phys. Rev. Lett. **46**, 1376 (1981).
- [6] J.J. Aubert et al., Phys. Lett. **B123**, 275 (1983).
- [7] R. Blankenbecler and S. Brodsky Phys. Rev. **D10**, 2973 (1974); G. Farrar and D. Jackson, Phys. Rev. Lett. **35**, 1416 (1975); A. Vainstein and V. Zakharov, Phys. Lett. **72B**, 368 (1978); D. Sivers Annu. Rev. Nucl. Part. Sci. **32**, 149 (1982).
- [8] A.I. Signal and A.W. Thomas, Phys. Lett. **B211**, 481 (1988); A.I. Signal and A.W. Thomas, Phys. Rev. **D40**, 2832 (1989); A.W. Schreiber, A.I. Signal and A.W. Thomas, Phys. Rev. **D44**, 2653 (1991).
- [9] A. Chodos, R.L. Jaffe, K. Johnson, C.B. Thorn and V.F. Weisskopf, Phys. Rev. **D9**, 3471 (1974).
- [10] M.R. Bate and A.I. Signal, J. Phys. G **18**, 1875 (1992).
- [11] R.E. Peierls and J. Yoccoz. Proc. Phys. Soc. **A70**, 381 (1957); R.E. Peierls and D.J. Thouless, Nucl. Phys. **38**, 154 (1962).
- [12] G. Altarelli and G. Parisi, Nucl. Phys. **B126**, 298 (1977).
- [13] R.S. Willey, Phys. Rev. **D18**, 270 (1978); P.M. Fishbane and M.T. Gisaru, Phys. Lett.

- 74B**, 98 (1978); S. Matsuyama and H. Miyazawa, Prog. Theor. Phys. **61**, 942 (1979); O.W. Greenberg and H.J. Lipkin, Nucl. Phys. **A370**, 349 (1981).
- [14] A. Schuh, H.J. Pirner and L. Wilets, Phys. Lett. **B174**, 10 (1986).
- [15] M. Bickeboeller, R. Goldflam and L. Wilets, J. Math. Phys. **26**, 1810 (1985); P. Tang and L. Wilets, J. Math. Phys. **31**, 1661 (1991).
- [16] M. Harvey, Nucl. Phys. **A352**, 301 (1981); *ibid.* 326.
- [17] T. Barnes, S. Capstick, M.D. Kovarik and E.S. Swanson, Phys. Rev. **C48**, 539 (1993).
- [18] R.L. Jaffe, Nucl. Phys. **B229**, 205 (1983).
- [19] K. Saito, A. Michels and A.W. Thomas, Phys. Rev. **C46**, R2149 (1992).
- [20] E. Naar and M.C. Birse, Phys. Lett. **B305**, 190 (1993).
- [21] F.E. Close and A.W. Thomas, Phys. Lett. **B212**, 227 (1988).
- [22] CTEQ Collaboration, Preprint MSU-HEP-41024 (1994), the CTEQ2M parameterization is used.
- [23] R. Kobayashi, M. Konuma and S. Kumano, Preprint SAGA-HE-63-94 (1994).
- [24] W. Koepf and L.L. Frankfurt, work in progress.
- [25] J. Kuti and V. Weisskopf, Phys. Rev. **D4**, 1400 (1981).
- [26] C.E. Carlson and T.J. Havens, Phys. Rev. Lett. **51**, 261 (1983).
- [27] K.E. Lassila and U.P. Sukhatme, Phys. Lett. **B209**, 343 (1988).
- [28] A.C. Benvenuti et al., Phys. Lett. **B189**, 483 (1987).
- [29] A. Bodek et al., Phys. Rev. Lett. **50**, 1431 (1983).